Dark matter or millisecond pulsars? A deep learning-based analysis of the Fermi Galactic Centre Excess

Florian List[1⋆, 2], Nicholas L. Rodd[3] and Geraint F. Lewis[2]

1 Department of Astrophysics, University of Vienna,
Türkenschanzstraße 17, 1180 Vienna, Austria
2 Sydney Institute for Astronomy, School of Physics, A28,
The University of Sydney, NSW 2006, Australia
3 CERN, Theoretical Physics Department, Geneva 1211, Switzerland

⋆ florian.list@univie.ac.at

Abstract

The γ-ray Galactic Centre Excess (GCE) remains one of the few observed high-energy signals for which a dark matter (DM) origin is a plausible explanation. We present a deep learning-based analysis of the γ-ray sky in the Galactic Centre region, carefully accounting for the mathematical degeneracy between faint point-sources (PSs) such as millisecond pulsars (MSPs) and DM-like Poisson emission. Using recent models for the Galactic foregrounds, we find that relatively few bright PSs just below *Fermi*'s detection threshold seem unlikely to explain the GCE, although we continue to find evidence for PSs. Looking ahead, further improvements in the modelling of the γ-ray sky will be crucial for distinguishing between a DM-like and point-like morphology of the signal.

Contents

1 Introduction

The Galactic Centre (GC) constitutes a prime target for indirect dark matter (DM) detection given its relative closeness to Earth and its high DM density (e.g. [1, 2]). Shortly after the launch of the *Fermi* satellite in 2008, an excess of photon counts from the vicinity of the GC was reported, for which DM annihilation was proposed as a possible explanation [3, 4]. In the past decade, this excess – known as the Galactic Centre Excess (GCE) – has been thoroughly scrutinised by numerous researchers, and its energy spectrum, spatial morphology, as well as luminosity seem to be largely consistent with an annihilation signature of weakly interacting massive particles (WIMPs), see e.g. [5–14]. However, astrophysical point-sources (PSs), each of them too faint to be individually resolved, provide an alternative explanation for the GCE (e.g. [15–21]). The arguments in favour of a PS explanation, most prominently a putative population of millisecond pulsars (MSPs), can generally be subdivided into two categories. First, there are claims that template fits exhibit a preference for the GCE to follow the stellar bulge rather than a squared Navarro–Frenk–White halo profile [22] as would be expected for DM annihilation [23–25] and second, some studies found a granular point-like GCE to be preferred over a smooth DM-like GCE morphology [26, 27]. Regarding the preference for the stellar bulge over a halo-like shape of the GCE, no final conclusions have been reached yet; for example, the recent studies in Refs. [13, 14] found good agreement with a DM-like distribution. For investigating the point-like vs. smooth (Poissonian) nature of the GCE – indicative of a PS or DM origin of the GCE, respectively – two methods have traditionally been used: the Non-Poissonian Template Fit (NPTF) [26, 28] (see also [29]) and wavelet analyses [27, 30, 31]. While early analyses using these methods obtained a strong preference for a point-like GCE [26, 27], doubt has been cast on the robustness of these results in Refs. [32–34], which demonstrated that a spurious preference for a point-like GCE may arise with the NPTF as an artefact of mismodelling the signal and backgrounds (see also Refs. [35] and [36] for discussions about the robustness of the NPTF). Further, a reanalysis of the *Fermi* data with the wavelet method by Ref. [37] identified a GCE consistent with Poisson emission when using an updated PS mask for the known bright sources [38].

In these proceedings, we will provide a brief synopsis of our work in Refs. [39, 40], where we demonstrated that convolutional neural networks (CNNs) [41] are a powerful alternative analysis method for the γ-ray sky, which appear robust to the systematic issues identified for the NPTF. In §2, we will introduce our analysis framework, followed by a brief summary of our main results in §3 and concluding remarks in §4.

2 Method

We model the γ-ray flux from the inner Galaxy region as a superposition of different emission components, each of which is described by an individual spatial template: (1) diffuse emission from pion decays and bremsstrahlung produced by the interaction of cosmic rays with the interstellar gas (π^0 + BS), (2) diffuse emission due to inverse Compton (IC) up-scattering of interstellar medium photons by cosmic-ray electrons, (3) isotropic emission originating from extragalactic sources, (4) the *Fermi* bubbles [42], (5) a PS population in the Galactic Disk, and (6) the GCE, which we model with a generalised NFW-squared profile with exponent $\gamma = 1.2$. For the disk PSs and the potentially point-like GCE, the exact locations of the individual sub-threshold sources are unknown, for which reason the resulting photon counts follow non-Poissonian statistics (see e.g. [26] for more details). In Refs. [39, 40], we considered the inner $\theta \leq 25°$ around the GC and masked latitudes $|b| \leq 2°$ as well as the resolved PSs in the 3FGL catalogue [43]. Our full data selection criteria are detailed in those works.

For our analysis of the *Fermi* data, we employ CNNs, which have become vastly popular across the sciences due to their ability to detect patterns in complex image data such as template edges and gradients for our task of disentangling γ-ray emission. While CNNs are arguably less interpretable than traditional analysis methods, they also possess notable advantages: first, CNNs assess entire *regions* of different sizes in γ-ray maps – in contrast to the product-over-pixel likelihood maximised by traditional template fitting methods, which may produce overly narrow posteriors because the counts in neighbouring pixels are in fact not independent of each other due to the point-spread function (PSF), which is what a product likelihood implicitly assumes (see Ref. [44]). This conceptual difference leads to a different behaviour of the methods in the presence of modelling deficiencies, see Ref. [40]. Second, as a representative of supervised machine learning methods, CNNs learn to infer the underlying relation between inputs (given by photon-count maps) and outputs from a labelled training dataset. Hence, the CNN can learn the effect of the PSF without being restricted by the need for explicitly prescribing an analytic approximation of the true likelihood. We take the label of each photon-count map to be the flux fraction of each template as well as the source-count distributions (SCDs) $F \frac{dN}{d \log_{10} F}$ of the PS templates (disk and GCE), which express the expected flux F of the dN PSs within each infinitesimal logarithmic flux bin $d \log_{10} F$.

We generate the training data by drawing from Poissonian distributions and using a modified version of `NPTFit-Sim` [45] for the Poissonian and PS templates, respectively. Importantly, we model all emission components that are *potentially* point-like as non-Poissonian. The rationale is as follows: Poisson emission can be viewed as the limit of $N \to \infty$ PSs that each contribute a negligible flux $F \to 0$ to the map, where the limit is taken such that $NF = \mu = \text{const}$. Thus, by choosing the priors for the SCDs in such a way that narrow SCDs peaking at very low fluxes corresponding to $\ll 1$ count per PS occur sufficiently often, many training maps will contain PS emission that is *virtually* indistinguishable from Poissonian emission. Using this approach, the (technically artificial) separation between Poissonian and point-like emission can be circumvented, acknowledging the fact that sufficiently faint PS emission is statistically degenerate with Poisson emission.[1]

Our analysis framework consists of two separate CNNs. The first CNN learns to estimate the flux fraction belonging to each template, disregarding whether the emission is Poissonian or point-like. Then, a second CNN is trained to predict the SCDs of the PS templates. For this purpose, we discretise the SCDs as histograms and utilise the Earth Mover's Pinball Loss function [46], which quantifies the uncertainties for the SCD histograms in terms of quantiles. Our CNN architecture is built on the graph-based `DeepSphere` framework [47, 48].

Finally, by comparing the predicted SCD for the *Fermi* GCE with our CNN predictions for simulated best-fit maps that contain an entirely Poissonian GCE, constraints on the Poissonian flux fraction of the *Fermi* GCE can be derived: GCE flux that the CNN attributes to bright PSs with high confidence is unlikely to have been produced by a Poissonian emission mechanism that follows the smooth NFW-squared template, whereas flux at the faint end of the estimated SCD cannot confidently be attributed to either dim PSs or Poissonian emission given their inherent degeneracy. For the full details of our methodology, we refer to Refs. [39, 40].

3 Results

Here, we present the main results derived from the *Fermi* data. Extensive experiments validating the performance of our CNN-based framework on simulated maps, as well as various

---

[1]Note that when modelling the Poissonian and PS components associated with one and the same spatial template separately instead (e.g. DM-like GCE and point-like GCE), particular care must be taken in order for the priors on the model parameters not to introduce a bias, see Ref. [44].

Table 1: Flux fraction estimates for each template (mean $\pm\, 1\sigma$, in %) in our region of interest ($\theta \leq 25°$, $|b| > 2°$, 3FGL masked) as determined by our CNN when modelling the diffuse emission with the model `p6v11` (for which all diffuse foregrounds are contained in a single template) and the more recent Model O.

	Diffuse π^0 + BS	Diffuse IC	Isotropic	*Fermi* bubbles	GCE	Disk
`p6v11`	88.5 ± 0.4		0.5 ± 0.4	6.3 ± 0.3	**4.4 ± 0.4**	0.5 ± 0.3
Model O	52.5 ± 0.9	26.6 ± 1.5	2.0 ± 0.9	5.9 ± 0.5	**7.4 ± 0.5**	5.7 ± 1.4

cross-checks for different template choices, the recovery of artificially injected GCE flux, and bias caused by different types of mismodelling can be found in Refs. [39,40].

Table 1 compares the flux fractions predicted by our CNN for two different choices of diffuse foreground models, the official *Fermi* model `p6v11` that was used in the original NPTF analysis by Ref. [26], and Model O, which was introduced in Ref. [36] (extending work by Refs. [23,49]) and has been shown to give a significantly better (albeit still suboptimal) fit to the *Fermi* data than `p6v11`. In particular, the overly hard IC component of `p6v11` at energies ≥ 10 GeV – which is fused with the diffuse foregrounds from pion decay and bremsstrahlung into a single template – may lead to over-subtraction of other emission components [11,36]. The results presented herein rely on the same priors for the data generation as in Ref. [39], but we binned the photon counts into `HEALPix` [50] pixels at resolution $N_{\mathrm{side}} = 128$ (instead of $N_{\mathrm{side}} = 256$ in that work). Notably, the flux assigned to the GCE increases by almost a factor of two when replacing `p6v11` with Model O, and much more flux is attributed to disk PSs. For completeness, we remark that the flux fraction estimates obtained with the `NPTFit` implementation [28] of the NPTF are very similar to those of our CNNs for both diffuse models (see Ref. [39]), demonstrating that the modelling uncertainties outweigh the differences between the results of the two methods.

Figure 1 shows our SCD estimates for the GCE, again for both diffuse models. Here, the difference is particularly striking: consistent with the original `NPTFit`-based analysis in Ref. [26], we identify a GCE PS population located not far below the *Fermi* detection threshold when using the diffuse model `p6v11`, implying that some hundreds to a few thousand relatively bright PSs would suffice to explain the GCE. However, with the more recent Model O, the SCD shifts to much fainter fluxes, peaking at a value corresponding to $3 - 4$ counts per PS with the data selection cuts in this present analysis. Importantly, for such a SCD, we cannot exclude that its low-flux end in fact represents Poissonian emission in view of the above-mentioned Poisson vs. dim PS degeneracy. Yet, also in this case the GCE was not found to be consistent with 100% Poissonian flux, and a PS contribution was required (see Ref. [40]).

4 Conclusions and outlook

In these conference proceedings, we have provided a bird's eye view of our machine learning-based framework for the analysis of the γ-ray sky presented in Refs. [39,40]. While modelling uncertainties still preclude a definite answer as to whether the GCE is caused by DM annihilation or by PSs such as MSPs, an important avenue is the development of novel analysis methods that – once the modelling of the γ-ray sky becomes sufficiently accurate – are able to accurately and reliably infer the GCE's flux, SCD, and energy spectrum. Importantly, since different analysis methods exhibit different systematics in the presence of modelling deficiencies (which can of course never be completely eradicated), taking the results of multiple methods in aggregate provides a more complete and in particular robust picture of the GCE's nature.
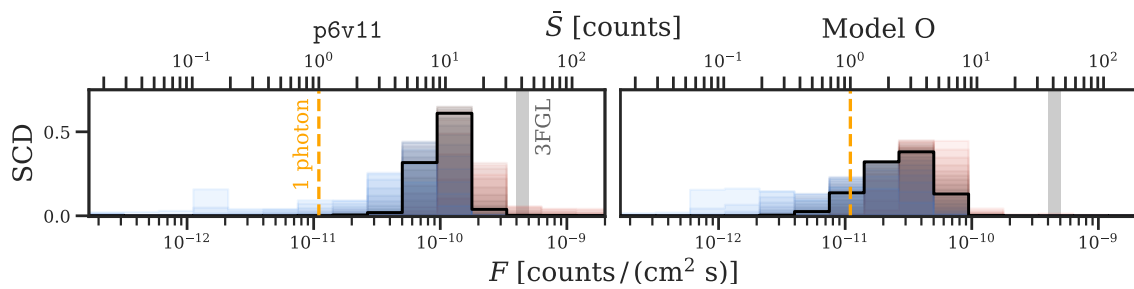
Figure 1: SCDs of the *Fermi* GCE estimated by our CNN for the diffuse model `p6v11` and Model O (arbitrarily normalised). Black lines show the median estimates, while the faint red to blue lines show 5%−95% quantiles. The flux corresponding to a single count per PS and the (approximate) *Fermi* 3FGL detection threshold are marked in the plot. The upper x-axis indicates the expected number of counts per PS.

A valuable extension of our method would be to consistently incorporate modelling uncertainties into our analysis by endowing templates with additional degrees of freedom (as done by e.g. Ref. [51] for a likelihood-based approach). In this spirit, Refs. [52, 53] recently explored the use of Gaussian Processes for making the diffuse emission model more flexible in the context of Normalising Flows.

Another possible refinement is to harness the spectral information alongside the photon-count statistics. So far, methods that attempt to distinguish DM from PSs based on photon-count statistics such as the NPTF or deep learning methods have analysed the *Fermi* data integrated over a certain energy range (e.g. $2 - 20$ GeV), thereby discarding the spectral information contained in the data (which, of course, has been the subject of other template-based analyses of the GCE, however, see e.g. Ref. [11]). This direction seems particularly promising because it would not only provide more nuanced information, but would also enable (1) the use of state-of-the-art templates that are tailored to specific energy ranges (e.g. [54]) and (2) a more accurate treatment of the *Fermi* PSF, which improves at higher energies.[2] With further progress on the modelling of the γ-ray sky, improvements in the analysis methods, and possibly the (non-)detection of the putative Galactic Bulge MSPs with upcoming radio telescopes, the 2020's will hopefully be the decade in which the GCE mystery is resolved.

References

[1] T. R. Slatyer, *Indirect detection of dark matter*, World Scientific, Singapore, ISBN 9789813233331 (2018), doi:10.1142/10798.

[2] S. Murgia, *The Fermi-LAT Galactic Center excess: Evidence of annihilating dark matter?*, Annu. Rev. Nucl. Part. Sci. **70**, 455 (2020), doi:10.1146/annurev-nucl-101916-123029.

[3] L. Goodenough and D. Hooper, *Possible evidence for dark matter annihilation in the inner Milky Way from the Fermi gamma ray space telescope*, (arXiv preprint) doi:10.48550/arXiv.0910.2998.

[4] D. Hooper and T. Linden, *Origin of the gamma rays from the Galactic Center*, Phys. Rev. D **84**, 123005 (2011), doi:10.1103/PhysRevD.84.123005.

---

[2] https://fermi.gsfc.nasa.gov/ssc/data/analysis/documentation/Cicerone/Cicerone_LAT_IRFs/IRF_PSF.html

[5] K. N. Abazajian and M. Kaplinghat, *Detection of a gamma-ray source in the Galactic Center consistent with extended emission from dark matter annihilation and concentrated astrophysical emission*, Phys. Rev. D **86**, 083511 (2012), doi:10.1103/PhysRevD.86.083511.

[6] D. Hooper and T. R. Slatyer, *Two emission mechanisms in the Fermi Bubbles: A possible signal of annihilating dark matter*, Phys. Dark Universe **2**, 118 (2013), doi:10.1016/j.dark.2013.06.003.

[7] C. Gordon and O. Macías, *Dark matter and pulsar model constraints from Galactic Center Fermi-LAT gamma-ray observations*, Phys. Rev. D **88**, 083521 (2013), doi:10.1103/PhysRevD.88.083521.

[8] K. N. Abazajian, N. Canac, S. Horiuchi and M. Kaplinghat, *Astrophysical and dark matter interpretations of extended gamma-ray emission from the Galactic Center*, Phys. Rev. D **90**, 023526 (2014), doi:10.1103/PhysRevD.90.023526.

[9] T. Daylan, D. P. Finkbeiner, D. Hooper, T. Linden, S. K. N. Portillo, N. L. Rodd and T. R. Slatyer, *The characterization of the gamma-ray signal from the central Milky Way: A case for annihilating dark matter*, Phys. Dark Universe **12**, 1 (2016), doi:10.1016/j.dark.2015.12.005.

[10] K. N. Abazajian, N. Canac, S. Horiuchi, M. Kaplinghat and A. Kwa, *Discovery of a new Galactic Center excess consistent with upscattered starlight*, J. Cosmol. Astropart. Phys. 13 (2015), doi:10.1088/1475-7516/2015/07/013.

[11] F. Calore, I. Cholis and C. Weniger, *Background model systematics for the Fermi GeV excess*, J. Cosmol. Astropart. Phys. 38 (2015), doi:10.1088/1475-7516/2015/03/038.

[12] T. Linden, N. L. Rodd, B. R. Safdi and T. R. Slatyer, *High-energy tail of the Galactic Center gamma-ray excess*, Phys. Rev. D **94**, 103013 (2016), doi:10.1103/PhysRevD.94.103013.

[13] M. Di Mauro, *Investigating the Fermi large area telescope sensitivity of detecting the characteristics of the Galactic center excess*, Phys. Rev. D **102**, 103013 (2020), doi:10.1103/PhysRevD.102.103013.

[14] M. Di Mauro, *Characteristics of the Galactic Center excess measured with 11 years of Fermi-LAT data*, Phys. Rev. D **103**, 063029 (2021), doi:10.1103/PhysRevD.103.063029.

[15] K. N. Abazajian, *The consistency of Fermi-LAT observations of the Galactic Center with a millisecond pulsar population in the central stellar cluster*, J. Cosmol. Astropart. Phys. 10 (2011), doi:10.1088/1475-7516/2011/03/010.

[16] K. N. Abazajian and M. Kaplinghat, *Detection of a gamma-ray source in the Galactic Center consistent with extended emission from dark matter annihilation and concentrated astrophysical emission*, Phys. Rev. D **86**, 083511 (2012), doi:10.1103/PhysRevD.86.083511.

[17] N. Mirabal, *Dark matter versus pulsars: Catching the impostor*, Mon. Not. R. Astron. Soc. **436**, 2461 (2013), doi:10.1093/mnras/stt1740.

[18] J. Petrović, P. D. Serpico and G. Zaharijas, *Millisecond pulsars and the Galactic Center gamma-ray excess: The importance of luminosity function and secondary emission*, J. Cosmol. Astropart. Phys., 23 (2015), doi:10.1088/1475-7516/2015/02/023.

[19] Q. Yuan and K. Ioka, *Testing the millisecond pulsar scenario of the Galactic center gamma-ray excess with very high energy gamma-rays*, Astrophys. J. **802**, 124 (2015), doi:10.1088/0004-637X/802/2/124.

[20] Q. Yuan and B. Zhang, *Millisecond pulsar interpretation of the Galactic center gamma-ray excess*, J. High Energy Astrophys. **3-4**, 1 (2014), doi:10.1016/j.jheap.2014.06.001.

[21] T. D. Brandt and B. Kocsis, *Disrupted globular clusters can explain the Galactic Center gamma-ray excess*, Astrophys. J. **812**, 15 (2015), doi:10.1088/0004-637X/812/1/15.

[22] J. F. Navarro, C. S. Frenk and S. D. M. White, *A universal density profile from hierarchical clustering*, Astrophys. J. **490**, 493 (1997), doi:10.1086/304888.

[23] O. Macias, C. Gordon, R. M. Crocker, B. Coleman, D. Paterson, S. Horiuchi and M. Pohl, *Galactic bulge preferred over dark matter for the Galactic centre gamma-ray excess*, Nat. Astron. **2**, 387 (2018), doi:10.1038/s41550-018-0414-3.

[24] R. Bartels, E. Storm, C. Weniger and F. Calore, *The Fermi-LAT GeV excess as a tracer of stellar mass in the Galactic bulge*, Nat Astron **2**, 819 (2018), doi:10.1038/s41550-018-0531-z.

[25] M. Pohl, O. Macias, P. Coleman and C. Gordon, *Assessing the impact of hydrogen absorption on the characteristics of the Galactic Center excess*, Astrophys. J. **929**, 136 (2022), doi:10.3847/1538-4357/ac6032.

[26] S. K. Lee, M. Lisanti, B. R. Safdi, T. R. Slatyer and W. Xue, *Evidence for unresolved γ-ray point sources in the inner Galaxy*, Phys. Rev. Lett. **116**, 051103 (2016), doi:10.1103/PhysRevLett.116.051103.

[27] R. Bartels, S. Krishnamurthy and C. Weniger, *Strong support for the millisecond pulsar origin of the Galactic Center GeV excess*, Phys. Rev. Lett. **116**, 051102 (2016), doi:10.1103/PhysRevLett.116.051102.

[28] S. Mishra-Sharma, N. L. Rodd and B. R. Safdi, *NPTFit: A code package for non-Poissonian template fitting*, Astron. J. **153**, 253 (2017), doi:10.3847/1538-3881/aa6d5f.

[29] D. Malyshev and D. W. Hogg, *Statistics of gamma-ray point sources below the Fermi detection limit*, Astrophys. J. **738**, 181 (2011), doi:10.1088/0004-637X/738/2/181.

[30] S. D. McDermott, P. J. Fox, I. Cholis and S. K. Lee, *Wavelet-based techniques for the gamma-ray sky*, J. Cosmol. Astropart. Phys., 45 (2016), doi:10.1088/1475-7516/2016/07/045.

[31] B. Balaji, I. Cholis, P. J. Fox and S. D. McDermott, *Analyzing the gamma-ray sky with wavelets*, Phys. Rev. D **98**, 043009 (2018), doi:10.1103/PhysRevD.98.043009.

[32] R. K. Leane and T. R. Slatyer, *Revival of the dark matter hypothesis for the Galactic Center gamma-ray excess*, Phys. Rev. Lett. **123**, 241101 (2019), doi:10.1103/PhysRevLett.123.241101.

[33] R. K. Leane and T. R. Slatyer, *Spurious point source signals in the Galactic Center excess*, Phys. Rev. Lett. **125**, 121105 (2020), doi:10.1103/PhysRevLett.125.121105.

[34] R. K. Leane and T. R. Slatyer, *The enigmatic Galactic Center excess: Spurious point sources and signal mismodeling*, Phys. Rev. D **102**, 063019 (2020), doi:10.1103/PhysRevD.102.063019.

[35] L. J. Chang, S. Mishra-Sharma, M. Lisanti, M. Buschmann, N. L. Rodd and B. R. Safdi, *Characterizing the nature of the unresolved point sources in the Galactic Center: An assessment of systematic uncertainties*, Phys. Rev. D **101**, 023014 (2020), doi:10.1103/PhysRevD.101.023014.

[36] M. Buschmann, N. L. Rodd, B. R. Safdi, L. J. Chang, S. Mishra-Sharma, M. Lisanti and O. Macias, *Foreground mismodeling and the point source explanation of the Fermi Galactic Center excess*, Phys. Rev. D **102**, 023023 (2020), doi:10.1103/PhysRevD.102.023023.

[37] Y.-M. Zhong, S. D. McDermott, I. Cholis and P. J. Fox, *Testing the sensitivity of the Galactic Center excess to the point source mask*, Phys. Rev. Lett. **124**, 231103 (2020), doi:10.1103/PhysRevLett.124.231103.

[38] S. Abdollahi et al., *Fermi Large area telescope fourth source catalog*, Astrophys. J. Suppl. Ser. **247**, 33 (2020), doi:10.3847/1538-4365/ab6bcb.

[39] F. List, N. L. Rodd, G. F. Lewis and I. Bhat, *Galactic center excess in a new light: Disentangling the γ-ray sky with Bayesian graph convolutional neural networks*, Phys. Rev. Lett. **125**, 241102 (2020), doi:10.1103/PhysRevLett.125.241102.

[40] F. List, N. L. Rodd and G. F. Lewis, *Extracting the Galactic Center excess' source-count distribution with neural nets*, Phys. Rev. D **104**, 123022 (2021), doi:10.1103/PhysRevD.104.123022.

[41] Y. Lecun, L. Bottou, Y. Bengio and P. Haffner, *Gradient-based learning applied to document recognition*, Proc. IEEE **86**, 2278 (1998), doi:10.1109/5.726791.

[42] M. Su, T. R. Slatyer and D. P. Finkbeiner, *Giant gamma-ray bubbles from Fermi-lat: Actice galactic nucleus activity or bipolar galactic wind?*, Astrophys. J. **724**, 1044 (2010), doi:10.1088/0004-637X/724/2/1044.

[43] F. Acero et al., *Fermi large area telescope third source catalog*, Astrophys. J. Suppl. Ser. **218**, 23 (2015), doi:10.1088/0067-0049/218/2/23.

[44] G. H. Collin, N. L. Rodd, T. Erjavec and K. Perez, *A compound Poisson generator approach to point-source inference in astrophysics*, ApJS **260**, 29 (2022), doi:10.3847/1538-4365/ac5cb7.

[45] N. Rodd and M. Toomey, *NPTFit-Sim*, GitHub (2017), https://github.com/nickrodd/NPTFit-Sim.

[46] F. List, *The Earth mover's pinball Loss: Quantiles for histogram-valued regression*, (arXiv preprint) doi:10.48550/arXiv.2106.02051.

[47] N. Perraudin, M. Defferrard, T. Kacprzak and R. Sgier, *DeepSphere: Efficient spherical convolutional neural network with HEALPix sampling for cosmological applications*, Astron. Comput. **27**, 130 (2019), doi:10.1016/j.ascom.2019.03.004.

[48] M. Defferrard, M. Milani, F. Gusset and N. Perraudin, *DeepSphere: A graph-based spherical CNN*, (arXiv preprint) doi:10.48550/arXiv.2012.15000.

[49] O. Macias, S. Horiuchi, M. Kaplinghat, C. Gordon, R. M. Crocker and D. M. Nataf, *Strong evidence that the galactic bulge is shining in gamma rays*, J. Cosmol. Astropart. Phys. 42 (2019), doi:10.1088/1475-7516/2019/09/042.

[50] K. M. Gorski, E. Hivon, A. J. Banday, B. D. Wandelt, F. K. Hansen, M. Reinecke and M. Bartelmann, *HEALPix: A framework for high-resolution discretization and fast analysis of data distributed on the sphere*, Astrophys. J. **622**, 759 (2005), doi:10.1086/427976.

[51] E. Storm, C. Weniger and F. Calore, *SkyFACT: High-dimensional modeling of gamma-ray emission with adaptive templates and penalized likelihoods*, J. Cosmol. Astropart. Phys. 22 (2017), doi:10.1088/1475-7516/2017/08/022.

[52] S. Mishra-Sharma and K. Cranmer, *Semi-parametric γ-ray modeling with Gaussian processes and variational inference,* (arXiv preprint) doi:10.48550/arXiv.2010.10450.

[53] S. Mishra-Sharma and K. Cranmer, *Neural simulation-based inference approach for characterizing the Galactic Center γ-ray excess,* Phys. Rev. D **105**, 063017 (2022), doi:10.1103/PhysRevD.105.063017.

[54] I. Cholis, Y.-M. Zhong, S. D. McDermott and J. P. Surdutovich, *Return of the templates: Revisiting the Galactic Center excess with multimessenger observations,* Phys. Rev. D **105**, 103023 (2022), doi:10.1103/physrevd.105.103023.